Available online at www.sciencedirect.com
SCIENCE DIRECT®
Bioelectrochemistry 60 (2003) 1–10
Bioelectrochemistry
www.elsevier.com/locate/bioelechem

Quantitative model of small molecules uptake after in vitro cell electropermeabilization

Marko Puc[a], Tadej Kotnik[a,b], Lluis M. Mir[b], Damijan Miklavčič[a,*]

[a] *Faculty of Electrical Engineering, University of Ljubljana, Tržaška 25, SI-1000 Ljubljana, Slovenia*
[b] *PPMB/UMR 8532 CNRS, Institute Gustave-Roussy, 39 rue C. Desmoulins, F-94805 Villejuif, France*

Received 24 September 2001; received in revised form 11 October 2002; accepted 17 December 2002

Abstract

Electropermeabilization of the cell membrane is a phenomenon caused by exposure of the cell to electric pulses. Permeabilization depends on pulse duration, pulse amplitude, the number of pulses delivered, and also on other experimental conditions. With these parameters properly chosen, the process of permeabilization is reversible and cells return to their normal physiological state. This article describes the development of a model of diffusion-driven transmembrane transport of small molecules caused by electropermeabilization. The process of permeabilization is divided into a short permeabilizing phase that takes place during the pulse, and a longer resealing phase that begins after the end of the pulse. Because both phases of permeabilization are important for uptake of molecules into cells, most of the effort is focused on the optimization of parameters that influence the flow between intracellular and extracellular space. The model describes well the transmembrane transport caused by electropermeabilization, allowing to study the uptake of molecules as a function of elapsed time, voltage and pulse duration. In addition, our results show that the shapes of the curves of cell permeabilization and survival as functions of pulse amplitude can to a large extent be explained by cell size distribution.

Keywords: Transmembrane transport; Electroporation; Electropermeabilization; Resealing kinetics; Pharmacokinetic model

1. Introduction

Electropermeabilization of the cell plasma membrane is a well-known phenomenon caused by exposure of cells to high-voltage electric pulses [1,2]. Permeabilization depends on pulse amplitude, pulse duration, number of delivered pulses, and also on other experimental conditions (temperature, osmotic pressure, etc.). With properly chosen values of the parameters of electric pulses, the process of electropermeabilization is reversible and cells return into their normal physiological state. If these parameters exceed certain values (e.g. amplitude of pulses is too high or duration of pulses is too long), cells are irreversibly permeabilized and lose their viability. The part of the plasma membrane that has been permeabilized by electric pulses provides the path for transport of different nonpermeant molecules into the cell. The quantity of molecules that will be introduced into the cell depends on their size, properties, extracellular concentration of molecules and on the degree of permeabilization (i.e. the change in diffusive permeability with respect to the normal state of the plasma membrane).

There are three general mechanisms of transport across a permeabilized membrane: diffusion, electrophoresis, and electroosmosis. During the pulse, once the membrane is permeabilized, these mechanisms can all contribute to the transport of molecules across the membrane, and the importance of each mechanism depends on the pulse length and amplitude, as well as on the type of molecule transported (see below). After the end of the pulse, until the membrane reseals completely, transmembrane transport of small molecules can only proceed by diffusion.

In the last decade, several studies have been published on the importance of each of the three transport mechanisms. Most of them imply that diffusion is the main component of transmembrane transport of small molecules [3–7], while electrophoresis can play a major role in

* Corresponding author. Tel.: +386-1-4768-456; fax: +386-1-4264-658.
E-mail address: damijan@svarun.fe.uni-lj.si (D. Miklavčič).

1567-5394/03/$ - see front matter © 2003 Elsevier Science B.V. All rights reserved.
doi:10.1016/S1567-5394(03)00021-5

transmembrane transport of macromolecules, particularly DNA [8–12]. We have recently indisputably demonstrated that electrophoresis is the most important mechanism of transport of DNA [13]. One report proposed electroosmosis as the dominating mechanism in transmembrane transport [14], but no other study supporting this opinion is known to the authors. The findings on importance of diffusion for small molecules, and of electrically driven transport for macromolecules also agree with the experimentally determined optimal pulse lengths for applications: hundreds of microseconds for small molecules, in contrast to tens of milliseconds for macromolecules. This suggests that with pulses lasting tens of milliseconds or longer, electrophoretic effect becomes sufficiently pronounced for electrically driven transport to play a major role. In the experiments on which our model is based (we used 100-μs pulses), the omission of electrically driven transport seems justified, particularly because, as we show in the results, even if Lucifer Yellow (LY) was added with a delay of 1 min after the pulse, the uptake exceeded 60% of that when LY was present when the pulses were delivered.

Our aim was to construct a model of diffusion-driven transmembrane transport on the basis of both theoretical and experimental work. The theoretical part of our study included the development of a dynamic model of diffusion-driven transmembrane transport caused by electropermeabilization. Values of parameters in the model were then estimated based on the experimentally determined percentages of permeabilized and surviving cells, as well as the average uptake of Lucifer Yellow per cell, each as a function of pulse amplitude and duration. This resulted in a quantitative model that is able to predict the quantity of molecules introduced by diffusion into the cell using specific pulse parameters. In addition, if the parameter describing the fast resealing of the membrane after the pulse is interpreted more generally, it can also incorporate electrophoretically and electroosmotically driven transport during the pulse.

Our experimental data also suggest that the variation of pulse amplitudes at which individual cells within the population are permeabilized, as well as the variation of pulse amplitudes at which individual cells lose their viability, can to a large extent be explained by the distribution of cell size within the population.

2. Experiments

2.1. Cells

DC-3F cells, a line of spontaneously transformed Chinese hamster fibroblasts [15], were grown in monolayers at 37 °C and 5% CO_2 in a Universal Jacketed Incubator (Forma Scientific, Marietta, OH, USA). Flasks (150 cm^2) were used for general cultivation, and 60 mm petri dishes were used for cloning efficiency assays (both from TPP, Trasadingen, Switzerland). The culture medium consisted of Eagle minimum essential medium (EMEM) 41090 supplemented with 10% fetal bovine serum (both from Life Technologies, Rockville, MD, USA), 100 U/ml penicillin and 125 mg/ml streptomycin (both from Sarbach/Solvay Pharma, Brussels, Belgium).

2.2. Exposure to electric pulses

After trypsination with trypsin-EDTA (Life Technologies), cells were centrifuged for 5 min at 1000 rpm in a C312 centrifuge (Jouan, Saint Herblain, France) and resuspended at 2×10^7 cells/ml in Spinner minimum essential medium SMEM 21385 (Life Technologies), which is a calcium-depleted modification of EMEM. A 50-μl droplet of the cell suspension was placed between two flat stainless steel electrodes 2 mm apart, and unipolar rectangular electric pulses were then applied with an electropulsator (GHT 1287B, Jouan). We applied a single pulse of 100 or 1000 μs duration at 10 amplitudes in a range from 0 to 400 V.

2.3. Determination of cell survival

Fraction of surviving cells was determined by their cloning efficiency. Cells were pulsed in suspension, under the conditions described above. After pulsation, cells were incubated for 10 min at room temperature and resuspended in SMEM. After additional 30 min, cells were transferred into the culture medium and grown for 5 days in 60 mm petri dishes (TPP, Trasadingen). Cells were then fixed with 100% ethanol (Carlo Erba Reagenti, Milan, Italy) and stained with 1% crystal violet (Sigma, St. Louis, MO, USA). Colonies were counted under a light microscope (Leica, Bensheim, Germany) and compared to the absolute control (unpulsed cells) to obtain the percentage of surviving cells.

2.4. Determination of cell permeabilization

Cell permeabilization was determined by means of bleomycin, a nonpermeant cytotoxic agent as described previously [16]. This method can be used because bleomycin at 5 nM concentration causes no statistically significant effect on cell survival in the absence of electric pulses. On the other hand this concentration is sufficient for lethal toxicity in electropermeabilized cells. Before pulsation, bleomycin (Laboratories Roger Bellon, France) was added to the suspension in the amount leading to 5 nM final concentration. After pulsation, cells were incubated for 10 min at room temperature and then diluted with 950 μl of SMEM to prevent drying. After an additional 30 min, cells were transferred into the culture medium and grown for 5 days in 60 mm petri dishes. Cells were then fixed with 100% ethanol and stained with

1% crystal violet. Colonies were counted and compared to the absolute control (unpulsed cells) to obtain the percentage of cells surviving the exposure to electric pulses in suspension with 5 nM bleomycin. By subtracting this percentage from 100%, the percentage of permeabilized cells was obtained.

2.5. Determination of Lucifer Yellow uptake

Average uptake per cell was determined by internalization of Lucifer Yellow CH dipotassium salt (LY, Sigma). The molecular weight (521.6 g/mol) of this molecule and its charge of -2 at complete dissociation are in the range of smaller drug molecules. Before pulsation, LY was added to the suspension to obtain 1 mM final concentration. After pulsation, cells were incubated for 10 min at room temperature and resuspended in SMEM. External LY was washed by two consecutive centrifugations and resuspensions in PBS. Cells were then broken down by ultrasonication (Sonifier 250, Branson, USA) and fluorescence was measured on spectrofluorometer (SFM 25, BioTek Kontron, France). Excitation was set at 418 nm wavelength and emission was detected at 525 nm. A calibration line was obtained by linear regression to the fluorescence of calibrating cuvettes containing 10 nM, 100 nM, and 1 μM LY. Concentrations of LY in the samples were determined based on this calibration curve.

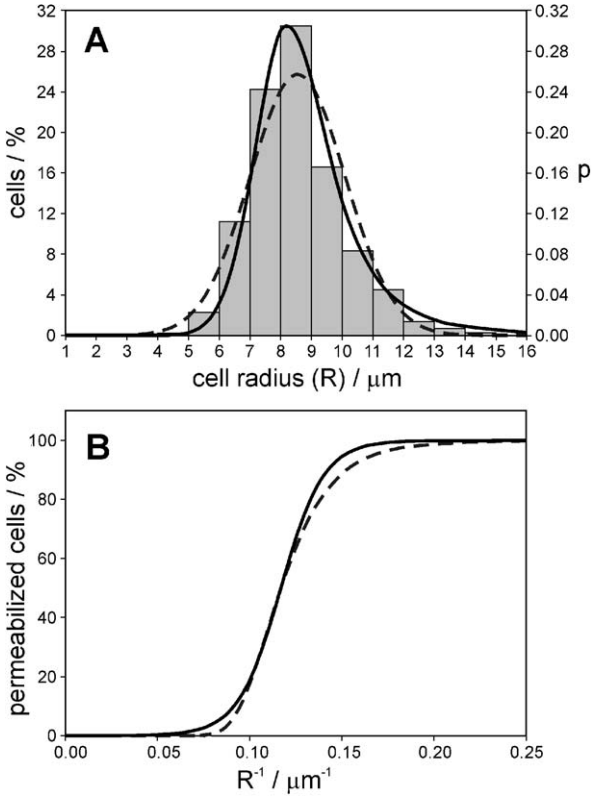

Fig. 1. The histogram in panel A shows the experimentally determined distribution of cell radii. The dashed curve in panel A is the hypothetical normal distribution of cell radii with the experimentally determined mean and standard deviation, and the dashed curve in panel B is the permeabilization curve which would follow from this distribution. The solid curve in panel B is the sigmoidal permeabilization curve obtained as the best fit to the experimental data, and the solid curve in panel A is the distribution of cell radii which would follow from this permeabilization curve if the distribution of cell radii would be the only reason for the dispersion of pulse amplitudes at which cells are permeabilized.

2.6. Determination of cell size

Average cell size was determined by measurements of cell diameter with DP 10 camera fixed on CK 40 microscope (both Olympus, Hamburg, Germany) at 200× magnification. Cell diameters were measured on three samples of cells (~15 cells in each sample) from cell suspension not exposed to electric pulses. In 448 measurements that we performed, we determined that cell radius varies in a range from 4 to 15 μm. The distribution of cell radii was in a good agreement with a normal distribution having the mean value 8.55 μm and standard deviation 1.55 μm (see Fig. 1).

3. Cell permeabilization and survival

Permeabilization of cell plasma membrane is achieved by application of electric pulses. The basic quantity underlying this process is the transmembrane potential difference induced by the electric field. For a cell with spherical shape (which is an acceptable approximation for most suspended cells), the induced transmembrane potential difference is described by [17]:

$$\Delta\Phi_{\mathrm{m}}(t) = f_{\mathrm{s}} ER\cos\theta\left[1 - \exp\left(-\frac{t}{\tau}\right)\right], \qquad (1)$$

where f_{s} is a function reflecting the geometrical and material properties of the cell and the surrounding medium [17], E is the amplitude of the electric field, R is the cell radius, θ is the polar angle measured with respect to the direction of the field, τ is the time constant of the inducement of transmembrane potential difference, and t is time elapsed from the onset of the electric field.

Under physiological conditions, the conductivity of the surrounding medium is several orders of magnitude larger than the conductivity of the cell plasma membrane, and the function f_{s} can be approximated by a constant, $f_{\mathrm{s}} = 3/2$, provided that the cell suspension is not too dense [18,19]. In addition, under physiological conditions, the time constant τ does not exceed 1 μs, while pulses typically used in electropermeabilization last for at least tens of microseconds. Thus, unless transient phenomena on the microsecond time scale are of interest, the exponential term in Eq. (1) can be omitted [17,20]. Most experimental con-

ditions used for electropermeabilization in vitro, including our experiments, are sufficiently close to physiological conditions to justify these two simplifications. Furthermore, when using two stainless steel parallel plate electrodes with plate sides substantially larger than the distance between them, the electric field strength E can be approximated by the voltage-to-distance ratio, U/d, where d is the electrode distance and U the pulse amplitude. At $\theta = 0°$, where the induced transmembrane potential difference is the largest, the described simplifications yield the following approximation of the expression (1):

$$\Delta\Phi_{\mathrm{m}} \doteq \frac{3UR}{2d}.$$

Provided that the value of the induced transmembrane potential difference that causes electropermeabilization is the same for all cells, and denoting this value by $\Delta\Phi_{\mathrm{mc}}$, it follows that for a cell with radius R, the voltage on the electrodes that causes permeabilization of this cell is given by

$$U_{\mathrm{c}} = \frac{2\Delta\Phi_{\mathrm{mc}}d}{3R}.$$

Our experiments have shown that the distribution of cell radii is in a reasonably good agreement with a normal distribution (see Section 2.6), for which the probability density p of a cell having a radius R would be given by

$$p(R) = \frac{1}{\sigma\sqrt{2\pi}}\exp\left(-\frac{(R-\bar{R})^2}{2\sigma^2}\right), \tag{2}$$

with $\bar{R}$ the average radius (experimentally determined $\bar{R} = 8.55$ μm) and σ the standard deviation ($\sigma = 1.55$ μm). This probability density, shown in dashed line in Fig. 1A, in which the experimental data are also shown in a histogram, would correspond to the probability of a cell having a radius larger than R_0

$$P(R \geq R_0) = \frac{1}{\sigma\sqrt{2\pi}}\int_{R_0}^{\infty}\exp\left(-\frac{(R-\bar{R})^2}{2\sigma^2}\right)dR. \tag{3}$$

Since this would equal the probability of a cell being permeabilized by the electrode voltage

$$U \leq \frac{2\Delta\Phi_{\mathrm{mc}}d}{3R_0},$$

the probability curve can also be plotted as a function of U, as shown in dashed line in Fig. 1B. Although this probability curve differs from a sigmoidal function (Fig. 1B, solid) which is often fitted to the experimental data, the difference is not substantial. The distribution of cell radii which would correspond to such a sigmoidal function is shown in Fig. 1A (solid), and even seems to agree better with the experimentally observed distribution of cell radii (Fig. 1A, the histogram).

With these considerations, we performed the analysis of cell survival and cell permeabilization fraction with respect to the distribution of cell size. Experimental results were fitted with two-parameter sigmoidal curves: cell permeabilization fraction (PF) as a function of voltage given by

$$\mathrm{PF}(U) = \frac{100\%}{1+\exp\left(-\dfrac{U-U_{50\%}}{b_{\mathrm{PF}}}\right)}, \tag{4}$$

and cell survival fraction (SF) as a function of voltage defined by

$$\mathrm{SF}(U) = \frac{100\%}{1+\exp\left(\dfrac{U-U_{50\%}}{b_{\mathrm{SF}}}\right)}. \tag{5}$$

In the process of curve fitting, we optimized parameters $U_{50\%}$, b_{PF}, and b_{SF} for each experiment, respectively. Voltages $U_{50\%}$ were then used to calculate the curves of cell permeabilization $\mathrm{PF_D}$ and cell survival $\mathrm{SF_D}$ fraction as a function of voltage using the equations:

$$\mathrm{PF_D}(U) = 100\% \cdot \begin{cases} 0 & U < U_{50\%} \\ 1 & U \geq U_{50\%} \end{cases}, \tag{6}$$

$$\mathrm{SF_D}(U) = 100\% \cdot \begin{cases} 0 & U \geq U_{50\%} \\ 1 & U < U_{50\%} \end{cases}, \tag{7}$$

As an alternative to the sigmoid fits, curves of cell permeabilization and cell survival following from a hypothetical normal distribution of cell radii (henceforth referred to as "normal distribution curves") were obtained from the step functions (6) and (7) by varying the cell radius according to this distribution, using the experimentally determined values of $\bar{R} = 8.55$ μm and $\sigma = 1.55$ μm. Fig. 2 compares the experimental data of permeabilization and survival with the best-fit sigmoidal curves and the normal distribution curves. The calculated goodness-of-fit between the normal distribution curves and the experiments (r_{n}^2), and between the fitted sigmoidal curve and the experiments (r_{s}^2) shows that both types of curves are in a good agreement with the experimental results. It would be difficult to decide which of the two types of curves is better suited to the description of experimental results, but these results nevertheless suggest that the dispersion of pulse amplitudes at which cells are permeabilized, as well as the dispersion of pulse amplitudes at which cells lose

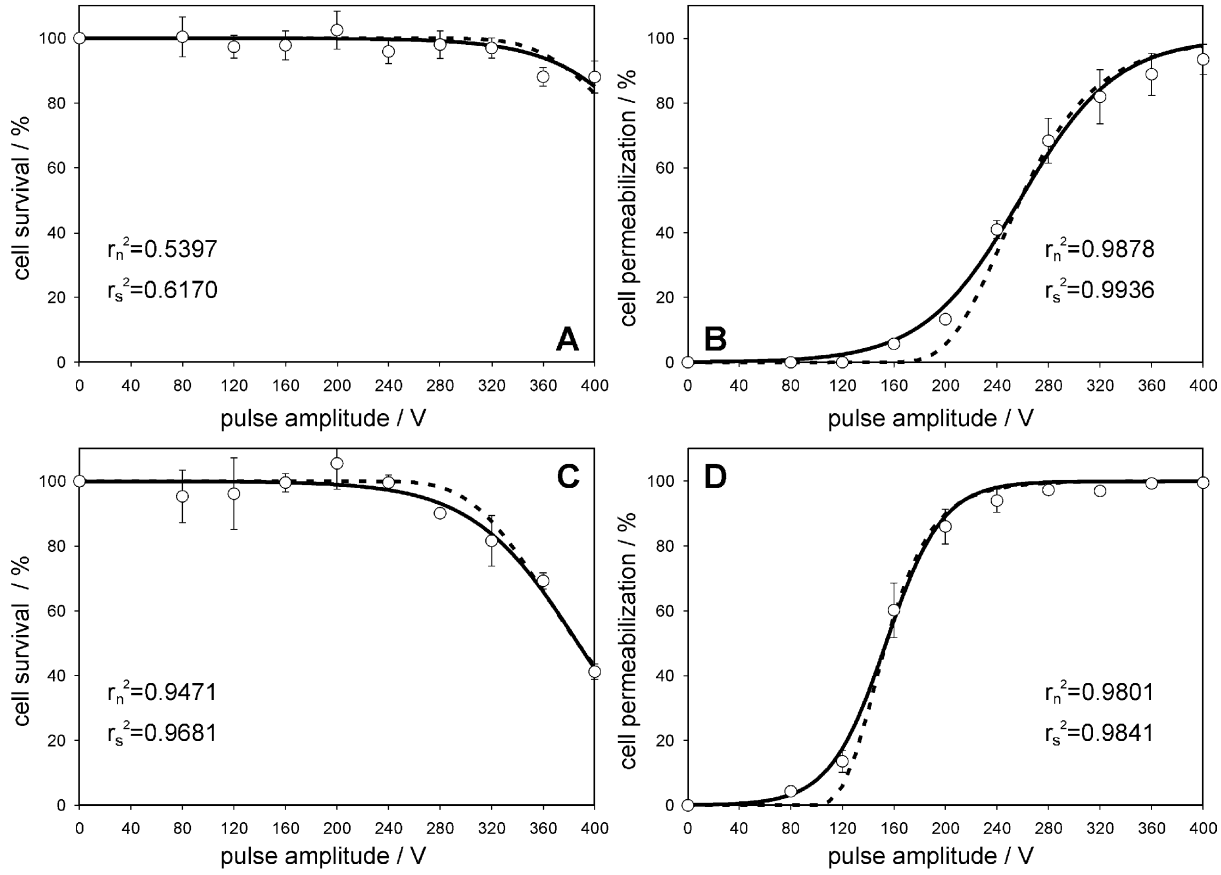

Fig. 2. The experimental data and the model curves of cell survival and cell permeabilization fraction as functions of pulse amplitude U. The circles (○) represent experimental results (mean ± S.D.), the dashed curves are the curves corresponding to a normal distribution of cell radii, and the solid curves are the best-fit sigmoidal curves. (A) Cell survival fraction for a single pulse of 100 μs ($U_{50\%}$ = 469 V), (B) cell permeabilization fraction for a single pulse of 100 μs ($U_{50\%}$ = 258 V), (C) cell survival fraction for a single pulse of 1000 μs ($U_{50\%}$ = 387 V), and (D) cell permeabilization fraction for a single pulse of 1000 μs ($U_{50\%}$ = 154 V).

their viability, can to a large extent be explained by the distribution of cell size (see Figs. 1 and 2).

4. Pharmacokinetic model of transmembrane transport

4.1. Development of the pharmacokinetic model

We performed measurements of the average uptake of Lucifer Yellow (LY) after electropermeabilization using single pulses of 100 and 1000 μs duration, at 10 different pulse amplitudes ranging from 0 to 400 V. In each experiment we followed the same protocol, from which we defined the following simulation parameters: external concentration 1 mM, resuspension time T_{10} = 10 min and the end of simulation T_{20} = 20 min. End time of simulation was set according to the previously published data by Neumann et al. [12].

We then constructed an isolated two-compartment pharmacokinetic model (Fig. 3), which describes transmembrane transport driven by diffusion and allowed us to calculate the quantity of molecules inside an average-sized cell. Mass transfer between the two compartments of the model shown in Fig. 3 is described by the following system of equations [21]:

$$\frac{dm_o}{dt} = -k_{oi}m_o + k_{io}m_i$$

$$\frac{dm_i}{dt} = k_{oi}m_o - k_{io}m_i, \quad (8)$$

where m_o and m_i are the masses of substance in each compartment that change with time (o stands for outside the cell and i stands for inside the cell), k_{oi} and k_{io} are coefficients describing the flow between the two compart-

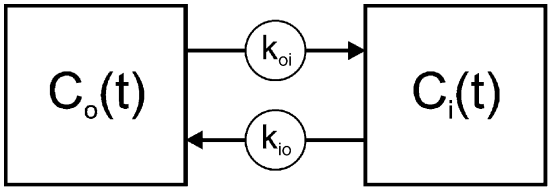

Fig. 3. The two-compartment pharmacokinetic model.

ments, and t is the time. Although this type of model deals with mass transfer, it can be easily transformed to concentration, since $m = CV$, where C is concentration in the compartment and V its volume. New system of equations that deals with concentrations thus reads:

$$\frac{dC_o}{dt} = -k_{oi}C_o + k_{io}\frac{V_o}{V_i}C_i$$

$$\frac{dC_i}{dt} = k_{oi}\frac{V_i}{V_o}C_o - k_{io}C_i. \quad (9)$$

In equilibrium, when concentration outside the cell is equal to the concentration inside the cell, both derivatives of concentration equal zero. This allows to define the relation between coefficients k_{io} and k_{oi}.

$$\frac{dC_o}{dt} = 0 \Rightarrow k_{oi} = k_{io}\frac{V_i}{V_o} \quad (10)$$

Thus we get:

$$\frac{dC_o}{dt} = k_{io}\frac{V_i}{V_o}(C_i - C_o)$$

$$\frac{dC_i}{dt} = k_{io}(C_o - C_i), \quad (11)$$

where C_o and C_i are external and internal concentration, respectively, k_{io} is a coefficient describing flow between the two compartments, V_o and V_i are volumes of compartments and t is time. However, as described above, electropermeabilization of the cell plasma membrane can be split into the permeabilizing phase that takes place during the pulse, and the resealing phase that begins after the pulse [6,11,12,22–24]. To simulate such behavior of the process of electropermeabilization, we introduced into the model (Fig. 4) a time variation of the coefficient k_{io} as follows:

$$k_{io} = \begin{cases} M & 0 < t \le T \\ gM\exp(\alpha(T-t)) & T < t \le T_{20} \end{cases}, \quad (12)$$

in which M is the flow coefficient [s^{-1}], α^{-1} is the time constant of resealing, g is a parameter that characterizes fast resealing immediately after the end of the pulse, T is the pulse duration and t is the time elapsed from the onset of the pulse. The values of $g = 0.5$ and $\alpha = 0.0038$ s^{-1} were determined from previously published data by Rols and Teissie [11] and Neumann et al. [12], while the value of M was investigated subsequently using our model. The role of parameter g can also be interpreted more generally, as incorporating, besides the fraction of transport that ceases after the fast resealing, also the electrophoretically and electroosmotically driven transport during the pulse.

Although Eqs. (11) and (12) allowed us to proceed with numerical optimization of parameters of the model, our aim was an explicit theoretical model. To achieve this, we made an additional simplification based on the experimental protocol and results. We assumed that until resuspension, external concentration of LY is constant (C_B) despite the uptake of molecules into the cell, and that after resuspension, C_o is zero and does not change despite possible release of molecules of LY from the cell that is still permeabilized. With this assumption we rewrote the equations of the model:

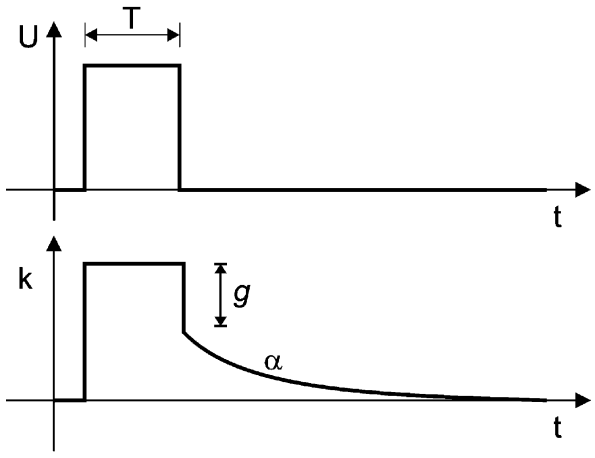

Fig. 4. The time course of the voltage applied to the electrodes, and the corresponding variation of coefficient k with time due to permeabilization and resealing of cell plasma membrane.

$$\frac{dC_i}{dt} = \begin{cases} k_{io}(C_B - C_i) & 0 < t \le T_{10} \\ -k_{io}C_i & T_{10} < t \le T_{20} \end{cases}. \quad (13)$$

Solution of this differential equation, assuming coefficient k_{io} varies with time according to Eq. (12), yields:

$$C_i(t) = \begin{cases} C_B[1 - \exp(-Mt)] & 0 < t \le T \\ C_B + (C_i(T) - C_B)\exp\left(-\frac{Mg}{\alpha}[1 - \exp(\alpha(T-t))]\right) & T < t \le T_{10} \\ C_i(T_{10})\exp\left(-\frac{Mg}{\alpha}[\exp(\alpha(T-T_{10})) - \exp(\alpha(T-t))]\right) & T_{10} < t \le T_{20} \end{cases}, \quad (14)$$

where C_i is the internal concentration, C_B the external concentration, T_{10} resuspension time, T_{20} duration of the simulation, and the other parameters are the same as in Eq. (12). Optimization of M was performed using experimental results from which we eliminated the influence of cell survival at different pulse amplitudes by calculating the ratio between the measured uptake of LY and the cell survival fraction at the same pulse amplitude. Optimization provided us with the values of M at different pulse amplitudes U, and these values were analyzed using the equation

$$M(U) = \frac{S(U)}{S_T}P(U), \quad (15)$$

where S is the permeabilization area of the plasma membrane, S_T is the total surface of the cell, and P is the degree of permeabilization of the area that defines the flow between

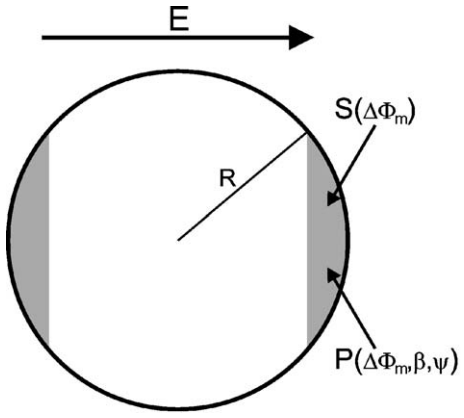

Fig. 5. Permeabilization of cell plasma membrane caused by applied electric field.

intracellular and extracellular space, and thus has the same unit as M [s^{-1}]. This interpretation was made because permeabilization of cell plasma membrane that is caused by externally applied electric field only occurs in those regions of the plasma membrane where the transmembrane potential difference, $\Delta\Phi_m$, exceeds a threshold value $\Delta\Phi_{mt}$ (Fig. 5). Area of the permeabilized plasma membrane, not taking into the account the resting membrane voltage, is given by [11,22]:

$$S = 4\pi R^2 \cdot \begin{cases} 0 & \Delta\Phi_m < \Delta\Phi_{mt} \\ 1 - \dfrac{\Delta\Phi_{mt}}{\Delta\Phi_m} & \Delta\Phi_m \geq \Delta\Phi_{mt} \end{cases} . \quad (16)$$

In our model, we used the value of $\Delta\Phi_{mt} = 250$ mV, according to Refs. [11,12]. The value of $\Delta\Phi_{mt}$ is considerably larger than the typical values of the resting transmembrane potential difference (tens of mV). In addition, due to the resting transmembrane potential difference, the total transmembrane potential difference is slightly higher at one pole of the cell, but lower by the same amount on the opposite pole (see Ref. [25] for details, including the analogue of Eq. (16) where the resting voltage is taken into account). Therefore, the effect of the resting transmembrane potential difference on the overall transport through the permeabilized membrane is not a significant one.

By defining the permeabilized area S and optimized maximal magnitudes of flow M at different pulse amplitudes we proceeded to reveal the function that would describe the degree of permeabilization P. In this process we fitted the function to the known points of P that were obtained from the ratio of optimized flow magnitudes M and size of permeabilized area S at identical pulse amplitudes. This function is given by:

$$P = \begin{cases} 0 & \Delta\Phi_m < \Delta\Phi_{mt} \\ \dfrac{\beta(T)}{T}\left[\exp(\psi(\Delta\Phi_m - \Delta\Phi_{mt})) - 1\right] & \Delta\Phi_m \geq \Delta\Phi_{mt} \end{cases} \quad (17)$$

where β and ψ are two parameters that were optimized and depend on pulse duration T. Their optimal values were $\beta = 12.223$, $\psi = 1.3503$ for 100 μs pulse duration, and $\beta = 249.85$, $\psi = 1.8591$ for 1000 μs pulse duration.

This completed the construction of our model. The input parameters of the model are: pulse amplitude (U), electrode distance (d), average radius of the cell (R), the inverse of the time constant of resealing (α), the fast-resealing parameter (g), the threshold value of transmembrane potential difference which leads to permeabilization ($\Delta\Phi_{mt}$), and extracellular concentration of the substance (C_B, in our case the concentration of LY).

4.2. Results obtained with the pharmacokinetic model

The pharmacokinetic model of transmembrane transport caused by electropermeabilization of cell plasma membrane described above allows to predict the uptake of small molecules as a function of electric field parameters, i.e.

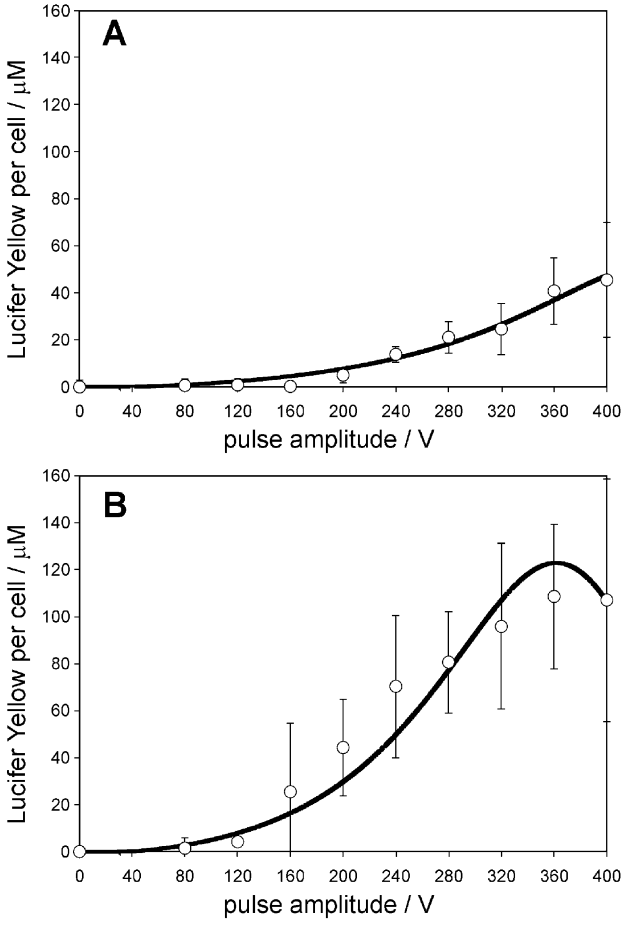

Fig. 6. Results of modeling of uptake of Lucifer Yellow (LY) as a function of pulse amplitude U. In both graphs circles (○) represent experimental results (mean ± S.D.) and solid line represents the course of uptake obtained by the model. (A) Uptake of LY for a single pulse of 100 μs, and (B) uptake of LY for a single pulse of 1000 μs.

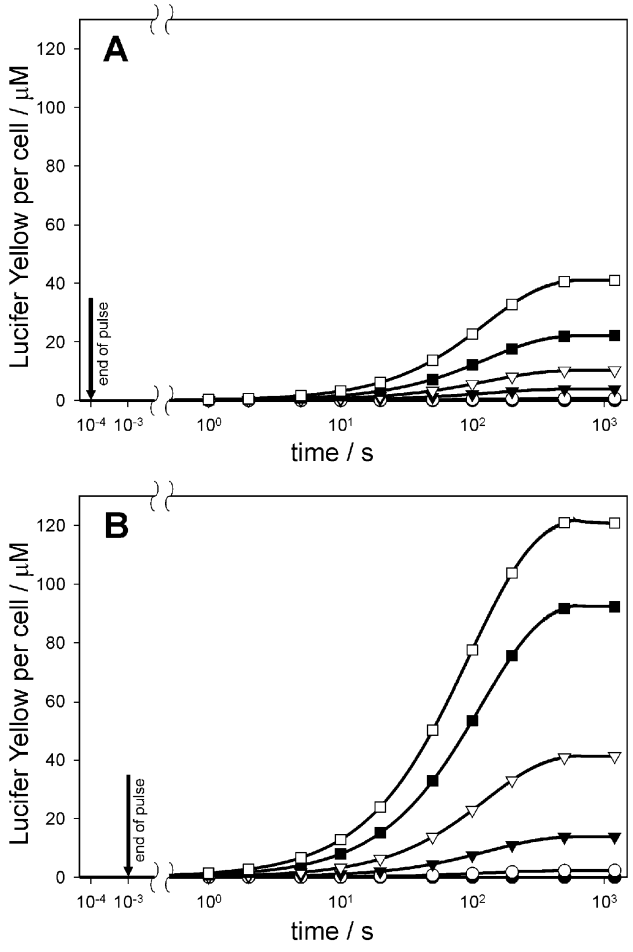

Fig. 7. Time course of LY uptake at different pulse amplitudes obtained by the model. (A) Uptake of LY for a single pulse of 100 μs, and (B) uptake for a single pulse of 1000 μs. Symbols on both graphs represent uptakes at following pulse amplitudes: (●) $U=0$ V, (○) $U=75$ V, (▼) $U=150$ V, (▽) $U=225$ V, (■) $U=300$ V and (□) $U=375$ V.

the amplitude and the duration of pulse (Fig. 6), as well as the uptake as a function of time at different parameters of electric field (Fig. 7).

5. Discussion

Electropermeabilization is widely used in different medical and biological applications such as electrochemotherapy, transdermal drug delivery, gene transfer, etc. [1,2]. Efficiency of all these applications depends on parameters of electropermeabilization that influence transmembrane transport and thus quantity of molecules that are introduced into the cells. With respect to this, optimal parameters for electropermeabilization have to be found to achieve best efficiency of the method. Optimization can be carried out with extensive experiments or with simulations with predictive model that is built on experimental and theoretical knowledge. Each approach has its advantages and disadvantages. Extensive experiments usually demand a lot of time and experimental material, but optimized parameters are gained on the real system [26]. On the other hand, simulations with predictive models can be performed at any time on computer, but the results of optimization depend on the robustness and adaptability of the model.

Simulations with our two-compartment pharmacokinetic model have shown that diffusion-driven transmembrane transport of small molecules into the average-sized cell can be quantified using this model. The model also allows to analyze the uptake of molecules into the cell as a function of elapsed time at different values of the pulse parameters (i.e. pulse duration and amplitude). Since the molecular weight and charge of LY are in the range typical for small molecules (see Section 2.5), the experimental results obtained with LY are likely to be rather representative for this class of molecules.

The development of the transmembrane transport model was based on the measurements of the uptake and cell survival at 100 and 1000 μs pulse durations. To predict the uptake at other pulse parameters, we have used linear interpolation and extrapolation to calculate parameters of the model. Fig. 8 shows results of simulations with the model at different values of the parameters of electric field (pulse width and amplitude).

Fig. 8 shows that our model predicts a plateau of uptake as a function of both pulse amplitude and duration, and such plateau was also observed experimentally [25,27]. To evaluate the predictive abilities of our model in more detail, two additional experiments were made subsequently, in which cells were exposed to a single pulse of 250 and 500 μs duration, respectively. For a 250 μs pulse with an amplitude of 320 V, the measured concentration of LY taken up per cell was 44.46 ± 7.30 μM (mean ± S.D.), while the prediction of the model is 42.31 μM. For a 500 μs pulse with an amplitude of 320 V, the experiment yields 62.72 ± 19.44 μM, and the model gives 67.45 μM. This shows that linear interpolation is an acceptable choice, and the predictive ability of the model is reasonably good at least for pulse durations in the range from 100 to 1000 μs.

The two-compartment pharmacokinetic model can be adapted to different experimental conditions. For example, we have set the external concentration C_B to 5 nM, which corresponds to the experimental conditions where we measured the permeabilization fraction by permeabilizing the cell in 5 nM concentration of bleomycin. To verify the model's adaptability, we used it to determine the number of molecules that are introduced into the average-sized cell. In the analysis of cell permeabilization performed using our model, the amount of molecules transported to the average-sized cell at pulse amplitude equal to $U_{50\%}$ is practically the same at any pulse duration (e.g. 122 molecules for $T=100$ μs and $U=258$ V; and 127 molecules for $T=1000$ μs and $U=154$ V). For bleomycin

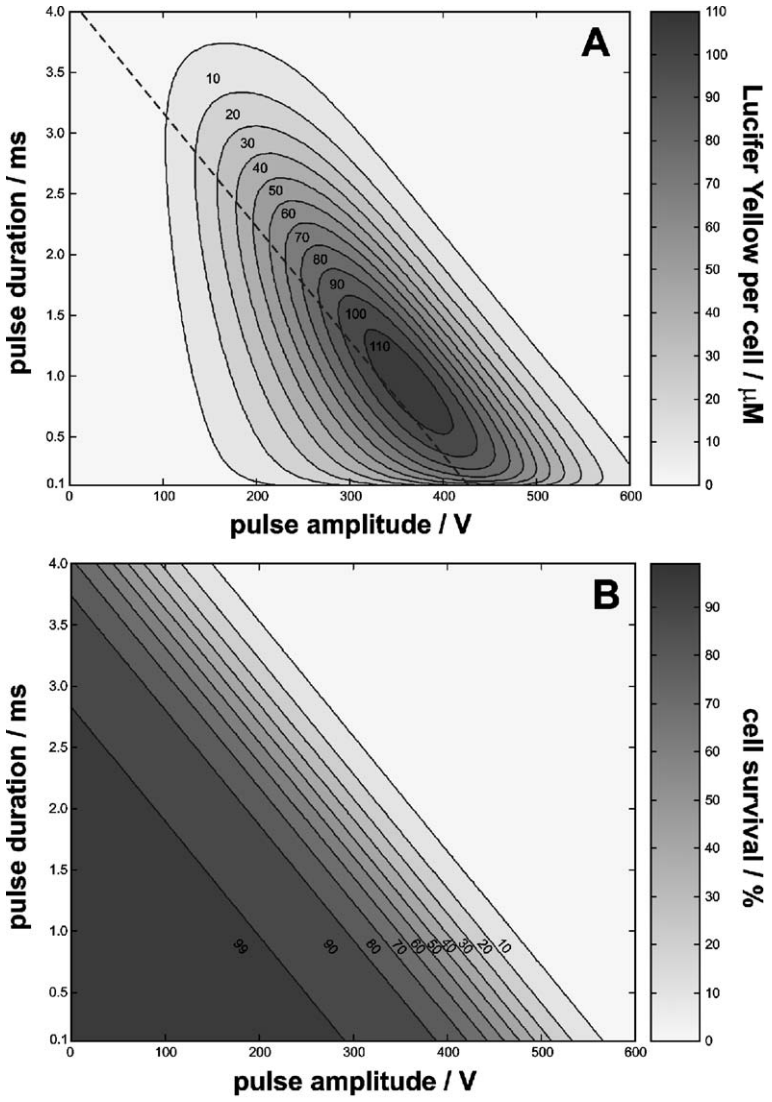

Fig. 8. Determination of optimal parameters to achieve greatest uptake taking into account also cell survival. Contour A shows uptake of LY as a function of pulse amplitude and pulse duration (β and ψ were linearly interpolated or extrapolated). The dashed line represents percentage of survived cells (in this case 78%) at different pulse parameters. Contour B shows the predicted cell survival as a function of pulse amplitude and pulse duration.

molecules experimental results published previously concluded that few hundred of molecules are sufficient to kill the cell [28,29], which is in the same order of magnitude as the data given by our model.

In the development of the pharmacokinetic model, the value of parameter g was interpreted as characterizing the fast resealing that takes place immediately after the end of the pulse. However, from a more general point of view, in addition to the fast resealing this parameter can be considered to incorporate the contribution of electrophoretically and electroosmotically driven transport. Disregarding inertia, these two components of transport also take place only during the pulse, and cease with its end.

Even though the molecular mechanisms of plasma membrane permeabilization are still not entirely clear, the data reported here show that it is possible to model adequately the transmembrane transport of small molecules through permeabilized cell plasma membrane.

Acknowledgements

This research has been supported through various grants by the Ministry of Education, Science and Sports (MESS) of the Republic of Slovenia. Experimental work in Villejuif (France) has been supported by grants of CNRS and the Institute Gustave-Roussy, while visits and stays have been made possible by the bilateral program of scientific, technological and cultural co-operation between CNRS (project No. 5386) and MESS (Proteus program). The authors wish to thank Dr. Maša Kandušer for cell size measurements, and Dr. Tomaž Jarm for

many useful suggestions during the preparation of the manuscript.

References

[1] L.M. Mir, Therapeutic perspectives of in vivo cell electropermeabilization, Bioelectrochemistry 53 (2000) 1–10.
[2] M.J. Jaroszeski, R. Heller, R. Gilbert, Electrochemotherapy, Electrogenetherapy, and Transdermal Drug Delivery, Humana Press, Totowa, 1999.
[3] E. Tekle, R.D. Astumian, P.B. Chock, Electropermeabilization of cell membranes: effect of the resting membrane potential, Biochem. Biophys. Res. Commun. 172 (1990) 282–287.
[4] E. Tekle, R.D. Astumian, P.B. Chock, Selective and asymmetric molecular transport across electroporated cell membranes, Proc. Natl. Acad. Sci. U. S. A. 91 (1994) 11512–11516.
[5] F.R. DeLeo, M.A. Jutila, M.T. Quinn, Characterization of peptide diffusion into electropermeabilized neutrophils, J. Immunol. Methods 198 (1996) 35–49.
[6] E. Neumann, K. Toensing, S. Kakorin, P. Budde, J. Frey, Mechanism of electroporative dye uptake by mouse B cells, Biophys. J. 74 (1998) 98–108.
[7] B. Gabriel, J. Teissie, Time course of mammalian cell electropermeabilization observed by millisecond imaging of membrane property changes during the pulse, Biophys. J. 76 (1999) 2158–2165.
[8] V.A. Klenchin, S.I. Sukharev, S.M. Serov, L.V. Chernomordik, Y.A. Chizmadzhev, Electrically induced DNA uptake by cells is a fast process involving DNA electrophoresis, Biophys. J. 60 (1991) 804–811.
[9] S.I. Sukharev, V.A. Klenchin, S.M. Serov, L.V. Chernomordik, Y.A. Chizmadzhev, Electroporation and electrophoretic DNA transfer into cells, Biophys. J. 63 (1992) 1320–1327.
[10] H. Wolf, M.P. Rols, E. Boldt, E. Neumann, J. Teissié, Control by pulse parameters of electric field-mediated gene transfer in mammalian cells, Biophys. J. 66 (1994) 524–531.
[11] M.P. Rols, J. Teissie, Electropermeabilization of mammalian cells to macromolecules: control by pulse duration, Biophys. J. 75 (1998) 1415–1423.
[12] E. Neumann, S. Kakorin, K. Toensing, Fundamentals of electroporative delivery of drugs and genes, Bioelectrochem. Bioenerg. 48 (1999) 3–16.
[13] S. Satkauskas, M.F. Bureau, M. Puc, A. Mahfoudi, D. Scherman, D. Miklavčič, L.M. Mir, Mechanisms of in vivo DNA electrotransfer: respective contributions of cell electropermeabilization and DNA electrophoresis, Mol. Ther. 5 (2002) 133–140.
[14] D.S. Dimitrov, A.E. Sowers, Membrane electroporation—fast molecular exchange by electroosmosis, Biochim. Biophys. Acta 1022 (1990) 381–392.
[15] J.L. Biedler, H. Riehm, Cellular resistance to actinomycin D in Chinese hamster cells in vitro, Cancer Res. 30 (1970) 1174–1184.
[16] T. Kotnik, A. Maček-Lebar, L.M. Mir, D. Miklavčič, Evaluation of cell membrane electro-permeabilization by means of a nonpermeant cytotoxic agent, Biotechniques 28 (2000) 921–926.
[17] T. Kotnik, F. Bobanović, D. Miklavčič, Sensitivity of transmembrane voltage induced by applied electric fields: a theoretical analysis, Bioelectrochem. Bioenerg. 43 (1997) 285–291.
[18] R. Susil, D. Šemrov, D. Miklavčič, Electric field induced transmembrane potential depends on cell density and organization, Electr. Magnetobiol. 17 (1998) 391–399.
[19] M. Pavlin, N. Pavšelj, D. Miklavčič, Dependence of induced transmembrane potential on cell density, arrangement, and cell position inside a cell system, IEEE Trans. Biomed. Eng. 49 (2002) 605–612.
[20] T. Kotnik, D. Miklavčič, T. Slivnik, Time course of transmembrane voltage induced by time-varying electric fields—a method for theoretical analysis and its application, Bioelectrochem. Bioenerg. 45 (1998) 3–16.
[21] M. Gibaldi, D. Perrier, Pharmacokinetics, Marcel Dekker, New York, 1975.
[22] M.P. Rols, J. Teissie, Electropermeabilization of mammalian cells. Quantitative analysis of phenomena, Biophys. J. 58 (1990) 1089–1098.
[23] M. Hibino, H. Itoh, K. Kinosita, Time course of cell electroporation as revealed by submicrosecond imaging of transmembrane potential, Biophys. J. 64 (1993) 1789–1800.
[24] M. Bier, S.M. Hammer, D.J. Canaday, R.C. Lee, Kinetics of sealing for transient electropores in isolated mammalian skeletal muscle cells, Bioelectromagnetics 20 (1999) 194–201.
[25] T. Kotnik, L.M. Mir, K. Flisar, M. Puc, D. Miklavčič, Cell membrane electropermeabilization by symmetrical bipolar rectangular pulses: Part I. Increased efficiency of permeabilization, Bioelectrochemistry 54 (2001) 83–90.
[26] P.J. Canatella, J.F. Karr, J.A. Petros, M.R. Prausnitz, Quantitative study of electroporation-mediated molecular uptake and cell viability, Biophys. J. 80 (2001) 755–764.
[27] M.R. Prausnitz, B.S. Lau, C.D. Milano, S. Conner, R. Langer, J.C. Weaver, A quantitative study of electroporation showing a plateau in net molecular transport, Biophys. J. 65 (1993) 414–422.
[28] B. Poddevin, S. Orlowski, J. Belehradek, L.M. Mir, Very high cytotoxicity of bleomycin introduced into the cytosol of cells in culture, Biochem. Pharmacol. 42 (1991) S67–S75.
[29] G. Pron, J. Belehradek, S. Orlowski, L.M. Mir, Involvement of membrane bleomycin-binding sites in bleomycin cytotoxicity, Biochem. Pharmacol. 45 (1994) 301–310.